Journal of Petroleum Science and Engineering 134 (2015) 49–59

Contents lists available at ScienceDirect

Journal of Petroleum Science and Engineering

journal homepage: www.elsevier.com/locate/petrol

Optimization of a CO_2 storage project based on thermal, geomechanical and induced fracturing effects

S. Goodarzi [a,*,1], A. Settari [a], M.D. Zoback [b], D.W. Keith [c]

[a] SPE, CGG, University of Calgary, Canada
[b] Stanford University, USA
[c] Harvard University, USA

ARTICLE INFO

Article history:
Received 24 October 2014
Received in revised form
30 May 2015
Accepted 2 June 2015
Available online 20 June 2015

Keywords:
CO_2 storage
Thermal
Geomechanics
Fracture
Thermoelasticity
Poroelasticity
Optimization

ABSTRACT

A coupled flow, geomechanical and heat transfer model for a potential CO_2 storage zone and surrounding formations has been developed. The coupled dynamic, thermal fracture model shows that thermal effects of injection could increase the speed of fracture propagation in the storage layer depending on the injection rate. Our work shows that the injection capacity with cold CO_2 injection could be significantly lower than expected, and it may be impractical to avoid induced fracture development. An optimization algorithm is proposed for maximizing the storage based on injection temperature while limiting the maximum fracture length and minimizing the risk of leakage from thermal effects of CO_2 storage while improving the injection capacity.

1. Introduction

Based on past sequestration pilot projects and enhanced oil recovery efforts, evidence suggests that geologic sequestration is a technically viable means to significantly reduce anthropogenic emissions of CO_2 (Solomon, 2006; Preston et al., 2005; Wright, 2007). Once CO_2 is injected, the pressure and temperature of the formation is affected by the mass and heat transfer between the injected and in place fluid. Cold CO_2 injection may have some advantages with respect to storage efficiency (Rayward-Smith and Woods, 2011; Silva et al., 2011).The pressure and temperature changes have geomechanical consequences on stresses, displacements, fracture pressure, and the fracture propagation. Since geomechanical effects induced by injection could lead to formation or reactivation of fracture network, rock shear failure and fault movements which could potentially provide pathways for CO_2 leakage, geomechanical modeling plays a very important role in risk assessment of geological storage of CO_2. Thermal effects of cold CO_2 injection has been studied by Goodarzi et al. (2011, 2012, 2013), Gor et al. (2013) and Peters et al. (2013). All the mentioned studies have shown stress reduction in the reservoir and caprock due to cold injection of CO_2. This reduction is due to rock thermal contraction resulting from heat transfer associated with cold injection of CO_2. The reduction of stresses has the potential to cause tensile fracturing in the reservoir and/or caprock as a result of lowered minimum effective stress (Goodarzi et al., 2011, 2012, 2013; Gor et al., 2013; Peters et al., 2013). This effect has been observed in one of the injection wells at In Salah (KB-502). Bissell et al. (2011) reported an abrupt increase in injectivity at a bottomhole pressure of 28.6 MPa (at 1330 m TVD) based on the injection data. This was interpreted as a sudden fracture opening and although this pressure is below the limit of the apparent fracture opening, the maximum well head pressure has been lowered at KB-502 (Rutqvist, 2012). Initiation of fracture below the apparent fracture opening pressure could be an indication of the cooling effects of CO_2 injection.

Goodarzi et al. (2011) have introduced the controversial idea of injecting CO_2 for storage at fracturing conditions in order to improve injectivity and economics. Here we examine the thermal aspects of such process. In order to test the effects of injection temperature on the increase of well injectivity under fracturing conditions, dynamic fracture propagation was modeled with accounting for both poroelasticity and thermoelasticity and the results were compared with corresponding study under isothermal condition. Finally an optimization methodology based on the

* Corresponding author.
E-mail addresses: sgoodarz@ucalgary.ca (S. Goodarzi), Tony.Settari@CGG.COM (A. Settari), zoback@stanford.edu (M.D. Zoback), david_keith@harvard.edu (D.W. Keith).
[1] Suite 1060, 1015-4th Street SW, Calgary, AB, Canada, T2R 1J4

http://dx.doi.org/10.1016/j.petrol.2015.06.004
0920-4105/

Nomenclature

$\$C_{energy}$	energy costs [$/KWh]
$\$C_{heating}$	heating costs [$]
$\$C_{pump}$	pumping costs [$]
C_p	heating capacity at supercritical condition [Kj/kg deg K]
ΔP	the pressure difference between the wellhead and the delivered pressure of CO_2 [kPa]
Q	injection rate [m^3/day]
Q_{cum}	total injected volume in each sector [m^3]
T	temperature [°C]
ΔT	temperature difference between the injection and the delivered temperature of CO_2 [°C]
ρ	density [kg/m^3]
η_p	pump efficiency
η_T	thermal efficiency of the heater
α	Biot constant

Subscripts

res	reservoir
inj	injection

injection temperature and fracture length has been proposed for maximizing the storage capacity while maintaining the security of storage.

Vilarrasa et al. (2014) have reported negative computed stress change in the injection zone after cold injection of CO_2 in the reservoir, in agreement with the other investigations. They however showed an increase in stresses in the caprock. This is an unexpected effect and needs further investigation.

With almost two hundred coal burning power plants in Ohio River Valley, located adjacent to the Mountaineer power plant in New Haven, West Virginia, this region is considered important for evaluation of CO_2 storage potential.

The study area is located in a relatively stable, intraplate tectonic setting and the regional stress state is in strike slip faulting regime with the maximum stress oriented northeast to east-northeast (Zoback and Zoback, 1981). Lucier et al. (2006) carried out a study for the Rose Run formation at the Mountaineer power plant in the Ohio River valley. After completing a geomechanical characterization of the Mountaineer site, Lucier et al (2006) simulated CO_2 injection into relatively low permeability Rose Run sandstone using a conventional reservoir simulator considering the pressure for fault reactivation as an upper boundary on reservoir pressures. Goodarzi et al. (2011) extended this previous study utilizing an isothermal reservoir model that explicitly couples pressure changes to geomechanics as CO_2 is injected using Geosim. GEOSIM™ is a modular software system that combines a 3D, 3-phase thermal reservoir simulator with a general 3D finite element stress–strain simulator (Taurus, 2015). The modular structure of the GEOSIM™ software allows flexibility in the level of coupling between the geomechanical and reservoir flow/heat systems. The details of the coupling have been described by Settari and Walters (2001). The software accounts for poroelastic and thermoelastic effects and can model static and/or dynamic fractures. The stress variation and displacement pattern under different CO_2 injection scenarios was investigated. In order to test the potential for increasing well injectivity, a static fracture with a half length of 300 m was introduced and its geomechanical consequences were analyzed. The scenario when the bottomhole pressure was allowed to exceed the fracture pressure (i.e., geomechanically coupled dynamic fracture propagation) was also modeled and the well injectivity was compared to that with a static fracture.

In this paper, Goodarzi et al. (2011) paper was extended by studying the thermal geomechanical effects of CO_2 injection in Rose Run sandstone aquifer located in the Ohio River Valley. This work used the fluid and rock mechanical properties provided in earlier publications (Lucier et al., 2006; Goodarzi et al., 2011). All the modeling was focused on a single well performance and considers induced fracturing for both isothermal and thermal injection conditions.

In order to test the effects of injection temperature on the increase of well injectivity under fracturing conditions, dynamic fracture propagation was modeled with accounting for both poroelasticity and thermoelasticity and the results were compared with our previous isothermal work. Finally an optimization methodology for maximizing storage capacity based on the injection temperature and fracture length has been proposed.

2. Coupled thermal and geomechanical model

The Rose Run sandstone (RRS), the potential injection zone at the Mountaineer site has an average 30 m thickness and is extended from 2355 to 2385 m depth (7728.4–7824.8 ft below ground surface). The stratigraphic sequence and the relative location of Rose Run to other formations can be seen in Fig. 1.

A quarter element of symmetry ($8000 \times 8000 \times 2575$ m^3) coupled geomechanical model ($40 \times 40 \times 9$ grid blocks) was built, with the injection well in the top left corner (Fig. 3). In order to avoid having initial non-zero shear stresses along the grid directions, all the model grids in this study are aligned along the maximum horizontal (N47E) and minimum horizontal (N43W) stress direction. Average properties of 5%, 20 md and 10 md for porosity, horizontal and vertical permeability were given to the injection layer. These values are the probability averages of the given property distributions for Rose Run sandstone formation (Lucier et al., 2006). The initial pressure and temperature of the RRS is 26,000 kPa and 63.1 °C. The fluid flow is simulated using a two-phase flow model with accounting for dissolution of CO_2 in water. The present work is focused on modeling of CO_2 injection through a single vertical well (below and above fracture pressure) for 30 years. To generate relative permeability data, Van Genuchten (1980) function was used with an irreducible gas saturation of 0.05, an irreducible liquid saturation of 0.2 and an exponent of 0.457.

Rose Run sandstone formation was gridded into 5 layers. In order to build the geomechanical model, the model grid was extended to include 3 upper layers (one layer from the surface to the top of the Trenton layer and two caprock layers: one for the Trenton and Black River limestone and the other one for Wells Creek and Beekmantown dolomite layer) and one bottom boundary layer (dolomite) (Refer to Fig. 1 for geological units and Fig. 3 for model layering).

The mechanical properties of the coupled model are listed in Table 1. The listed values are extracted directly from the Lucier et al. paper with the exception of grain modulus. Grain modulus was back-calculated from the Biot constants and Young's Moduli reported in Lucier et al. (2006). The Biot constant α is important for computing the effects of pressure changes on stress. At the Mountaineer site, Lucier et al. estimated α to be very low – in the

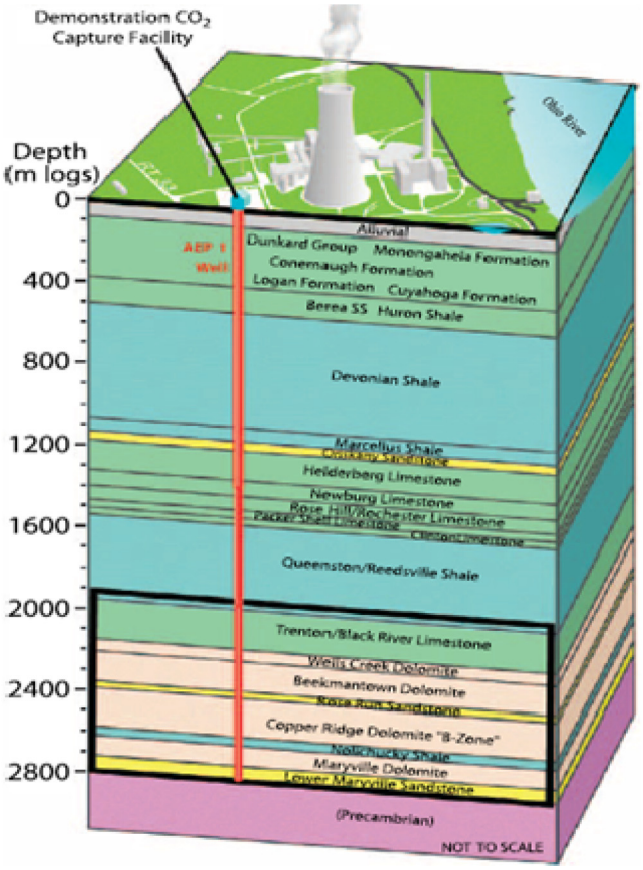

Fig. 1. Generalized stratigraphy of the study site. The well location and the general stratigraphy intersected by well is illustrated in the picture. The black box shows the boundaries of the area of previous work by Lucier et al. (2006), modified from Gupta (2008).

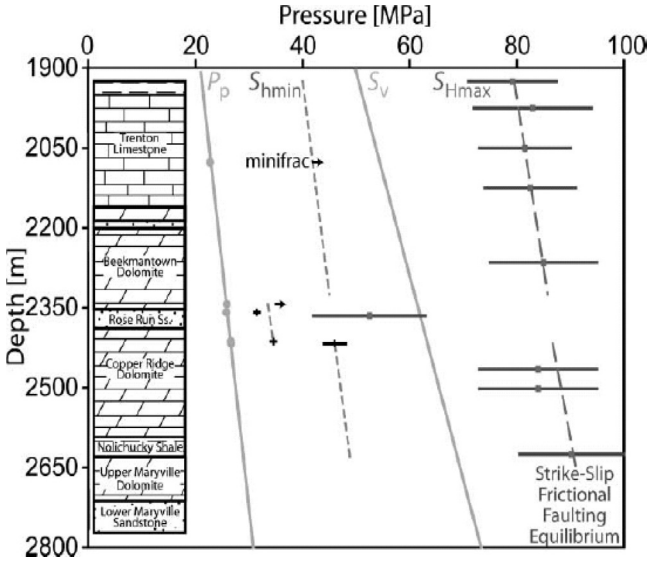

Fig. 2. Pressure and stress magnitudes with depth in the Ohio River Valley (Lucier et al. 2006).

range of 0.03–0.2. In this analysis, a mean value of 0.11 was used to calculate the poroelastic effects.

Fig. 2 shows the pressure, horizontal and vertical stress magnitude for different formations at different depths in the Ohio River Valley. It is important to note that the horizontal stresses in the injection layer (RRS) are lower than in the surrounding layers.

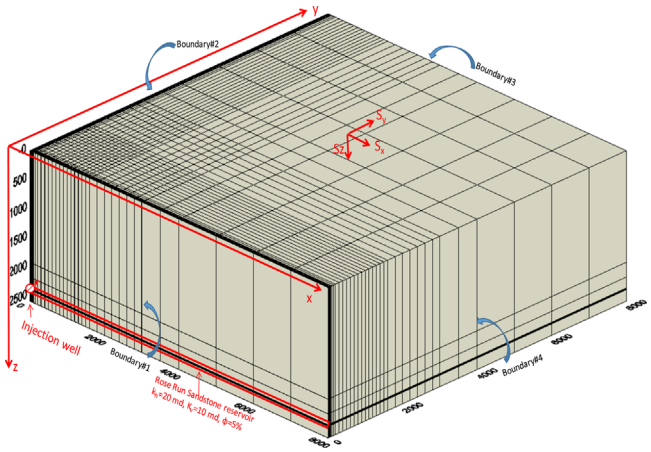

Fig. 3. 3D geomechanical grid marked with the injection well location in the reservoir and stress directions.

In many situations the stresses in caprock (low permeability rock) are larger than in the reservoir (permeable formations), because of differences in Poisson's ratio, material properties, stress history and other factors. This is well documented in hydraulic fracturing literature and is the primary mechanism for containment of fractures to the target zone. Having a larger magnitude of stresses in the caprock will decrease fracture propagation through the caprock. If sufficient stress contrast exists, it would limit the fracture growth into the caprock, and therefore increase the injectivity of reservoir (by fracturing) without endangering the security of storage. This stress state is very critical when considering fracturing the reservoir layer while preventing fracture growth through upper caprock layers. Fig. 3 shows the 3D geomechanical grid marked with the injection well location in the reservoir and stress directions. The layers shown in this figure correspond to the layer numbers in Table 1.

Since cold CO_2 (at approximately 30 °C) will likely be injected into the relatively hot Ohio formation (at 60 °C), thermal effects of injection on fluid flow and geomechanics should be included in the model. The thermal properties used for models in this study are listed in Table 2 (Collieu et al., 1975[3]; Fjaer et al., 2008[2]; Guildner, 1958[5]; Lucier et al., 2006[1]; Yaws, 2008[4]). The volumetric thermal expansion coefficient of CO_2 is calculated internally based on Charles's gas law and the input PVT table which is derived from Hassanzadeh et al. (2008).

3. Modeling approach for coupled flow, thermal and geomechanical model

The numerical methods for solving the fluid flow, energy and geomechanical equations are Finite Difference and Finite Element methods respectively. The two models are explicitly coupled (on a time step basis), i.e. once the fluid flow and energy equations have been solved for the increments of pressure and temperature over a time step, these two variables for each grid block will be sent to the geomechanical model in order to solve the solid mechanics equations for strains and to update the stresses. Then, the new stresses will be used to calculate the stress dependent permeability modifiers for the fractured grid blocks in order to model fracture propagation for the next time step in the flow model. Therefore, the geomechanical model which couples the flow, thermal and stress module is extended to include modeling of dynamic fracture initiation and propagation. In order to consider the dynamic propagation of a tensile fracture, a plane of grid cells is first designated as a potential fracture plane. Then,

Table 1
Rock mechanical properties of the coupled model.

Geological unit-top depth (m)	Model layer numbers	Thickness (m)	Young's Modulus (kPa)	Poisson's Ratio	Grain Modulus (KPa)
Shale-Surface	1	1911	6.00E+07	0.29	5.25E+07
Limestone-1911	2	253	7.05E+07	0.3	6.61E+07
Dolomite-2164	3–5	186	8.96E+07	0.28	7.51E+07
Rose Run Sandstone-2350	6–8	30	8.73E+07	0.25	6.53E+07
Dolomite-2380	9	195	9.47E+07	0.28	8.05E+07

Table 2
Thermal properties of fluids and rock.

	Rock	Water	CO_2
Volumetric thermal expansion coefficient (1/ K)	5.4E−6[1]	2.1E−4[2]	3.003E−3
Heat capacity (kJ/(kg K))	0.9[2]	4.182[2]	0.84[3]
Thermal conductivity (W/m K)	2.34[1]	0.65[4]	0.084[5]

transmissibility multiplier functions are dynamically computed for each interblock connection in this fracture plane, as a function of effective stress perpendicular to this plane. This models the effect of fracture opening on fluid flow, which in turn will change the stresses around the fracture through poroelasticity.

In order to calculate the functions, an assumption of fracture half height (in case of a vertical fracture) is required. It should be noted that the function theoretically increases without limit as pressure in the fracture increases and effective stress decreases. However, the function should be bounded in practice, since the effect of further increase of the conductivity of the fracture becomes negligible beyond some value (i.e., infinite conductivity is reached) which can be determined by sensitivity analysis. Limiting the conductivity (or transmissibility) is necessary for maintaining the numerical stability. If the fracture height exceeds the assumed height used, the actual multipliers would be higher, but this representation is still a good approximation for the reasons stated above. In addition, one can also compute the effect of the fracture width on the porosity of the block that has been fractured.

This method has been shown to be accurate and equivalent to more rigorous hydraulic fracture modeling methods for problems dominated by leak-off (Ji et al., 2004). The technique is further discussed in Goodarzi et al. (2011). The stress convention in this study is that compressive stresses are positive and tensile stresses are negative.

4. Thermal effects of injection below fracturing pressure

In order to study thermoelastic effects of injection, thermal equations were incorporated into already existing coupled model (Goodarzi et al., 2011). This model has a constant pressure boundary condition and CO_2 is injected through a single well at the top left corner under a maximum bottomhole pressure constraint of 32,000 kPa. The maximum bottomhole pressure is selected based on targeting injection below fracturing pressure. Fig. 4 shows the pressure and temperature distribution at the reservoir's top layer after 30 years of injection. It should be noted that the temperature distribution is illustrated on a 600×600 m^2 area zoomed around the well in order to see the influenced region. This shows a significantly smaller area under thermoelastic influence of CO_2 injection relative to the area affected by poroelasticity.

Injecting cold CO_2 will reduce the stresses in the injection layer and once the temperature front has reached a relatively large area around the wellbore, the reduction in stresses will cause negative volumetric strains which get transferred to the surface. The surface displacements for the thermal model will therefore fall below that of the isothermal model. Fig. 5 compares the vertical surface displacement at the top left corner (Fig. 3) for the thermal and isothermal model. Thermal models in this paper refer to models having lower injection temperature than the reservoir temperature (60 °C). In isothermal models, injection temperature is equal to reservoir's temperature.

One of the most important effects of injection of cold CO_2 is on the fracture pressure. Cooling of the formation reduces the total stresses and therefore lowers the fracture propagation pressure.

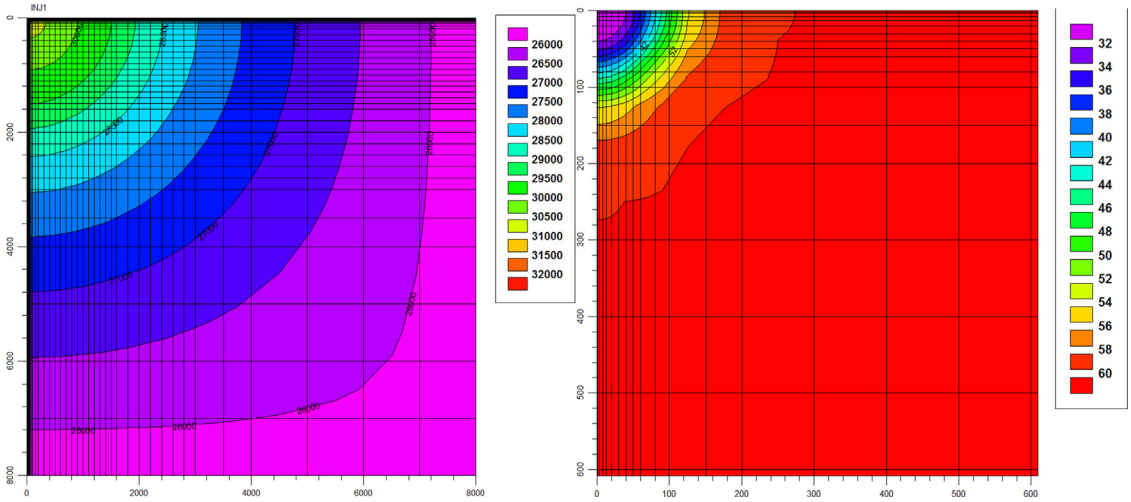

Fig. 4. Pressure distribution (left) and temperature distribution (zoomed to 600×600 m^2 area around the wellbore) (right) at reservoir's top layer after 30 years of injection in the case of injection below fracture pressure (35,000 kPa) with constant bottomhole pressure of 32,000 kPa and injection temperature of 30 °C, and constant pressure boundary condition at the right and front side of the model.

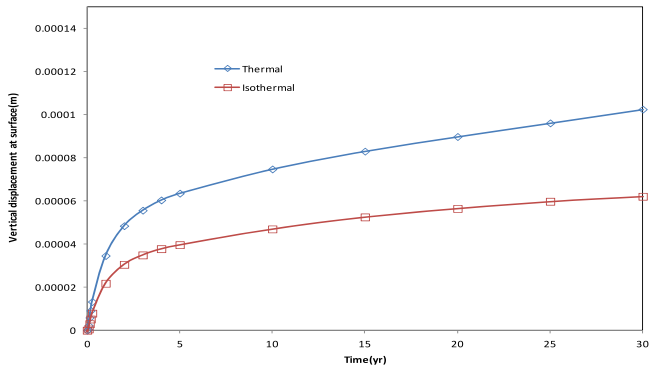

Fig. 5. Surface displacement (m) at the top left corner (Fig. 3) for the thermal and isothermal model in the case of injection below fracture pressure (35,000 kPa) with constant bottomhole pressure of 32,000 kPa and constant pressure boundary condition.

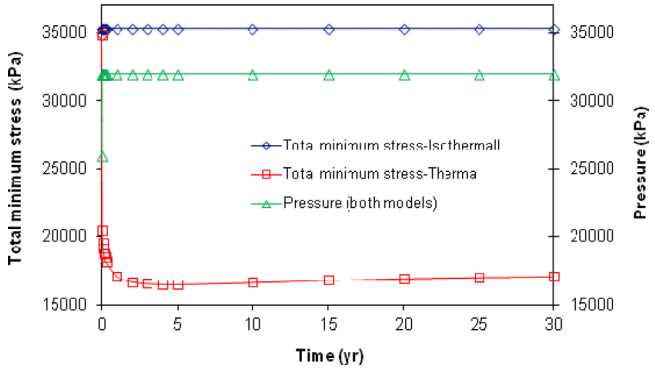

Fig. 6. Total minimum stress and pressure history for the wellblock at reservoir's topmost layer in the case of injection below initial fracture pressure (35,000 kPa) with constant bottomhole pressure of 32,000 kPa and constant pressure boundary condition.

In the case of injection at fracturing conditions, the fracture propagation pressure will decrease and this reduces the pressure differential available for injection, and therefore injectivity. However, if the same injection rate is used, this will accelerate fracture propagation and longer fracture length will increase injectivity. Fig. 6 shows the variation of the total minimum stress and pressure for injection below fracture pressure for both isothermal and thermal case. In both cases, injection was forced at constant pressure below the initial minimum stress, but fracture propagation was not allowed in the modeling. As it is seen, the total stress falls below the pressure for the thermal model at quite early injection times which means that minimum effective stress will reduce below zero. Therefore, although CO_2 is injected below the original fracture pressure, fracture would in reality initiate in the thermal model. It is important to stress again that the stress magnitudes after the indicated onset of fracturing are not valid in this example. However, this comparison demonstrates how quickly fracturing condition can be reached.

The injected volume of CO_2 for the thermal model without fracturing was 9E3 m^3. This is much lower than the injected volume for the isothermal model without reaching tensile fracturing (3.5E8 m^3) and shows a significantly lower storage capacity for injection below fracture pressure when considering thermal effects of injection.

5. Thermal effects on dynamic fracturing

Thermoelastic stress change resulting from injection of CO_2 with a lower than reservoir temperature is an important factor that contributes to spontaneous tensile fracturing. Extensive experience with water injection into reservoirs and aquifer disposal zones has shown that many injectors will experience spontaneous fracturing even when the well is operated below the initial fracture pressure (Settari and Warren, 1994). Although this creates some risks concerning the security of storage (primarily about fracture containment), operating at fracturing pressure enhances injectivity and therefore should be considered for CO_2 storage projects.

For modeling the dynamic propagation of fracture, a plane of grid cells is first designated as the potential fracture plane. An effective-stress-dependent transmissibility multiplier function was dynamically computed for grid cells in the designated potential fracture plane extending from the wellblock. The derivation of the transmissibility and porosity multiplier functions can be found in Goodarzi et al. (2011). Thermal effects of injection on the dynamic fracture can be seen by studying the fracture length, vertical growth, and fracture propagation pressure. In order to study these effects of injection on fracture propagation, the model was run with a constant injection rate increased to 7.2E4 m^3/day. With this injection rate, the bottomhole pressure reaches the fracture pressure with both isothermal and thermal models.

The properties used for dynamic fracture model in the isothermal model are described in Goodarzi et al. (2011). The outer right boundary conditions (boundaries#3 and 4 shown in Fig. 3) of this model were initially constant pressure in order to have a comparison with the models in Goodarzi et al. (2011), but changed later as will be discussed below. Based on the assumed symmetry, a no-flow condition was imposed across left boundaries (boundaries#1 and 2 shown in Fig. 3). The dynamics of the fracture propagation is complex as it depends on both poroelastic and thermoelastic effects on stresses. Fig. 7 shows the fracture length and bottomhole pressure for thermal and isothermal injection of CO_2 with 7.2E4 m^3/day under constant pressure boundary condition. Well block pressure is very close to the bottomhole injection pressure. As expected, for the isothermal model, due to pressure support from boundary blocks, once the pressure front reaches the boundaries of the model (constant pressure condition), the boundary pressure support and increased gas relative permeability in the free gas zone lead to reduction of pressure in the fracture and shrinkage of fracture length. However, in the thermal model due to reduced temperature area around the well, even with the boundary pressure support, since thermal stresses are reduced around the well, the fracture length remains almost constant after 5 years of injection.

In field CO_2 storage projects, more than a single well is drilled in the targeted formation and constant pressure boundary condition would not be a realistic condition for modeling multi-well injection scenario. Therefore the boundary condition was changed to a no-flow boundary condition so that the repeated well pattern

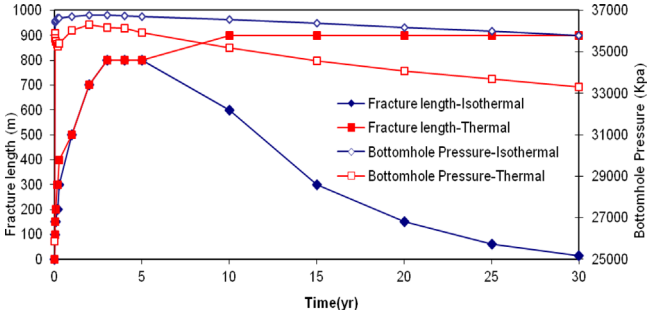

Fig. 7. Fracture half length and bottomhole pressure for thermal and isothermal injection of CO_2 with 7.2E4 m^3/day injection rate with constant pressure boundary condition.

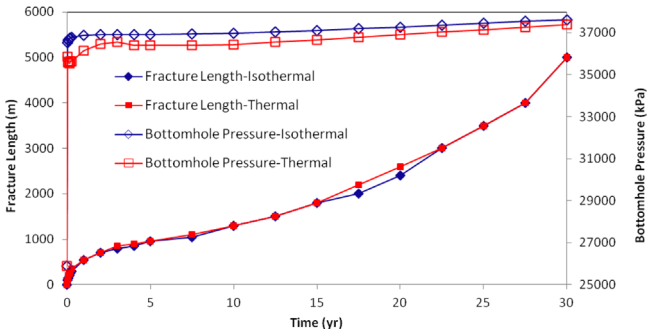

Fig. 8. Fracture half length and bottomhole pressure at well for thermal and isothermal model with 7.2E4 m^3/day injection rate with no-flow boundary condition.

could be better simulated. Also in order to estimate the fracture length more accurately, a refinement in simulation time and grid (around the wellbore) was implemented. The number of grid blocks after this refinement is $50 \times 50 \times 9$. Fig. 8 compares the fracture length and bottomhole pressure for the thermal and isothermal model. The bottomhole pressure for these two models is very close to the bottomhole injection pressure at which the fracture propagates. Since thermoelastic effects reduce stresses around the well, fracture propagates at lower pressure for the thermal model compared to the isothermal model. However due to the domination of poroelastic over thermoelastic effects, the reduction in the fracturing pressure is small, and fracture length is affected very little by thermal effects. The fracture lengths for the two models are almost the same throughout the injection history. However, it should be kept in mind that the resolution of the fracture length is limited to a grid block size, and that will be more apparent in the following cases where fracture lengths are smaller.

If the injection rate is reduced, heat transfer will start to dominate the geomechanical effects of injection and fracture propagation. Therefore, due to thermal stress reduction, fracture length for thermal model will be higher than for the isothermal model. Fig. 9 shows the wellblock pressure and fracture length for thermal and isothermal model for two different smaller injection rates. As seen, the difference between the fracture length of the thermal and isothermal model increases as the injection rate is reduced. In general, one expects that the thermal effect of injection on fracture propagation is a function of pressure diffusivity, thermal diffusivity and injection rate.

Since the horizontal stresses in the Rose Run reservoir are much lower than in the surrounding layers, vertical propagation of fracture in the caprock does not occur either for the thermal or isothermal model. However, if the stress contrast does not exist, thermal effects on height growth can be important,-as shown in a feasibility study of CO_2 storage in Wabamun lake area in Canada (Goodarzi et al., 2012). Thermal effects of injection are also important for evaluating the chance of reaching shear failure in the caprock (Goodarzi et al., 2013).

The lack of smoothness seen on Fig. 9 is caused by the resolution of the length being limited by the grid block size. It is worth noting that in the model the fracture propagates through a fixed grid. In order to get more accurate results, one would need to build a model with different grid for each case, compatible with the expected fracture growth. In this work, we have chosen to use a common grid in order to facilitate comparison, but this aspect will be studied further.

6. Thermal effects on fracture length

If thermoelasticity is the driving mechanism for fracture propagation, as the injection temperature reduces, the fracture length increases. Fig. 10 shows the fracture length for injection temperatures of 30, 45, and 60 °C and injection rates of 4.5E4 m^3/day and 5E4 m^3/day. As the injection rate decreases and thermoelasticity dominates, the difference between the fracture length of the isothermal model and thermal model increases.

7. Poroelasticity vs thermoelasticity

The phenomenon of the competition between poro and thermoelasticity described above can be clearly seen in Figs. 11 and 12. These two figures show pressure, temperature and minimum effective stress distribution at reservoir's top layer for injection at two different rates. The model is a ¼ element of symmetry (for details see Goodarzi et al., 2011). These two sets of figures are both zoomed on the near-well area with the well in the upper left corner, and with a linear *x*-scale magnified to the fracture length at the end of injection, and *y*-scale being logarithmic.

Effective stress distribution in both Figures shows negative values along the fracture length. However, for the higher injection rate (Fig. 12), temperature front is much more behind the pressure front and therefore pressure is the main driving mechanism for fracture propagation and varying temperature does not much affect the fracture length.

Heat transfer mechanisms are heat convection and diffusion. Fracture propagation strongly influence heat convection and temperature distribution. The relationship between heat diffusion and convection and the competition between them is complex and need to be studied further.

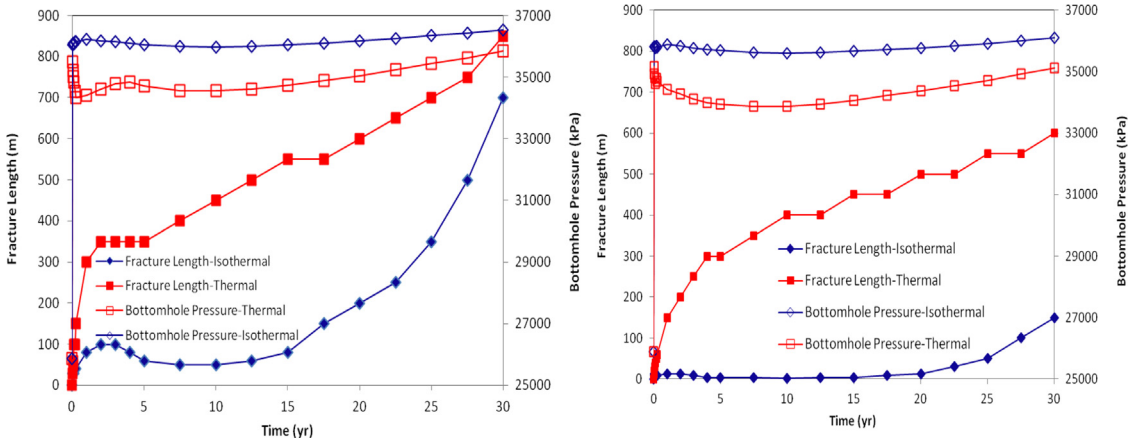

Fig. 9. Fracture half length and bottomhole pressure with no-flow boundary condition with 5E4 m^3/day injection rate (left) and with 4.5E4 m^3/day injection rate (right).

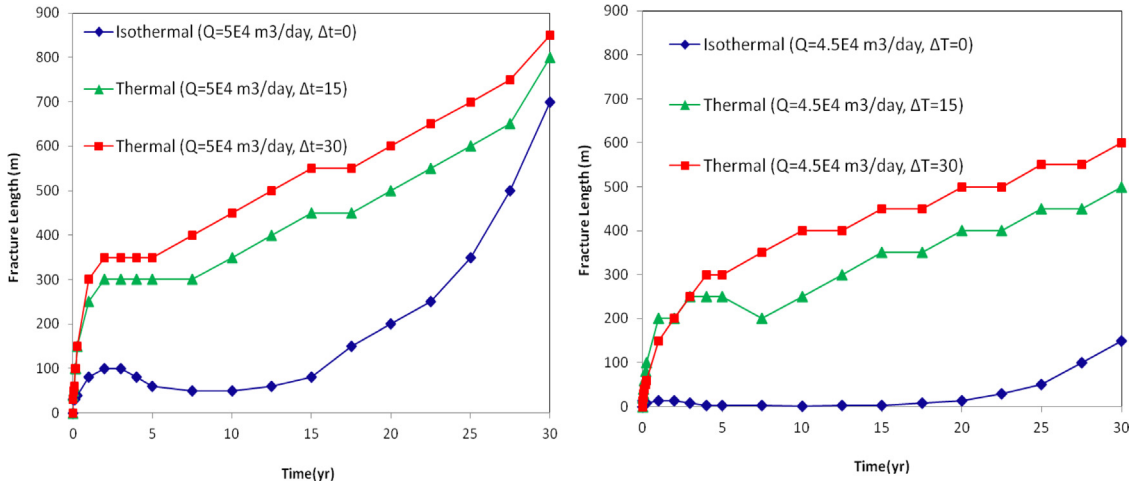

Fig. 10. Effect of injection temperature on fracture length for thermal model with 5E4 m^3/day (left) and 4.5E4 m^3/day injection rate (right).

Fig. 13 shows total minimum stress, pressure and temperature distribution along the fracture plane for the low (4.5E4 m^3/day) and high (7.2E4 m^3/day) injection rate case after 30 years of injection. The fracture tip for both cases is at the point where the pressure and total minimum stress curves coincide. As can be seen in both cases, the pressure gradient in the fracture plane is very small and the pressure drops considerably beyond fracture tip.

In the low injection rate case the temperature front is at fracture tip (~600 m) and therefore controlling the propagation and shows considerable difference around the tip. In contrast, in the high injection rate case, the temperature front is far behind the fracture tip (~5000 m) and does not have any effect on the propagation.

8. Optimization possibilities

The concept demonstrated above is potentially very important for CO_2 storage optimization process because injection temperature can be controlled. The simulations show that the thermal effects on fracture length are only significant at sufficiently small injection rates. Despite the small injection rate, fracture will be initiated due to thermal effects of cold CO_2 injection. At high rates, fracture propagation will occur regardless of the injection temperature. It is therefore expected that in CO_2 injection, we will have to deal with fracturing in most cases, except for very low rates which will maintain injection pressure below the reduced stresses in fully cooled target zone.

Given that the injection pressure, fracture propagation and length depends on injection temperature, the well injectivity, which is determined by the difference between the injection and far field reservoir pressure and fracture length, will also become a function of temperature. The wellhead injection temperature itself is a function of the temperature of the source, process used to capture and transport the CO_2, geographical location and etc. The cost of transporting CO_2 to the wellhead is also a function of many variables such as CO_2 phase and density. The temperature of the CO_2 in the pipeline determines its density and volume, and therefore affects the compressor horsepower and pipeline diameter needed. The CO_2 Capture and Storage (CCS) project can be designed such that the injection temperature is controlled by cooling or heating. Therefore, injection rate and temperature should be both considered as optimization variables. Optimizing the storage process can be based on maximizing the injectivity while maintaining the security of storage. This second criterion is complex in itself and involves interaction with other wells through propagating fractures as well as caprock integrity issues. For the purpose of this study we have represented this criterion simply by limiting the fracture length, because the caprock integrity issues in the study area are not significant.

At injection rates at which thermal effects are important, if injected CO_2 has a lower temperature than reservoir temperature, in order to keep the fracture at a given maximum length, either the injection rate must be decreased or CO_2 has to be heated to higher temperature before injection. Higher temperature means higher capital and operating costs for transportation and injection. On the other hand, injecting CO_2 at smaller rates with a fixed

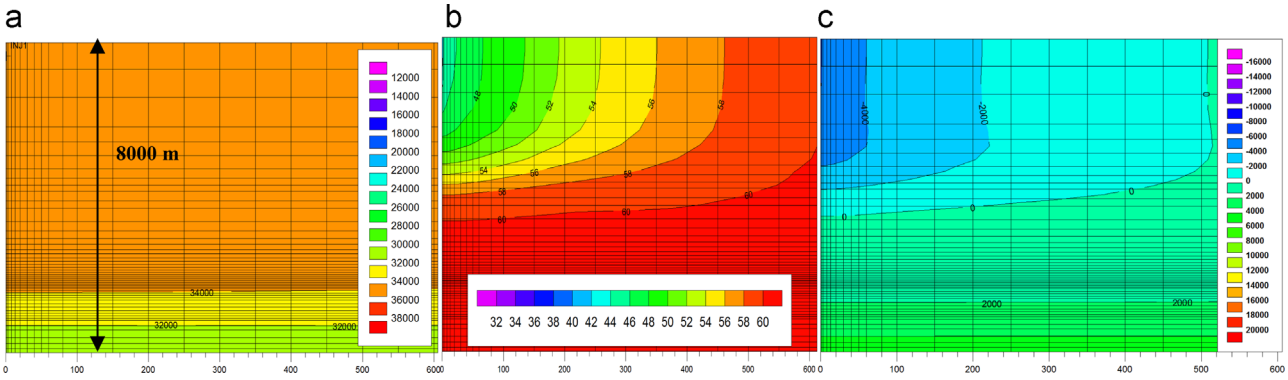

Fig. 11. (a) Pressure (kPa) distribution, (b) temperature (°C) and (c) minimum effective stress (kPa) after 30 years of injection for thermal model with 4.5E4 m^3/day injection rate.

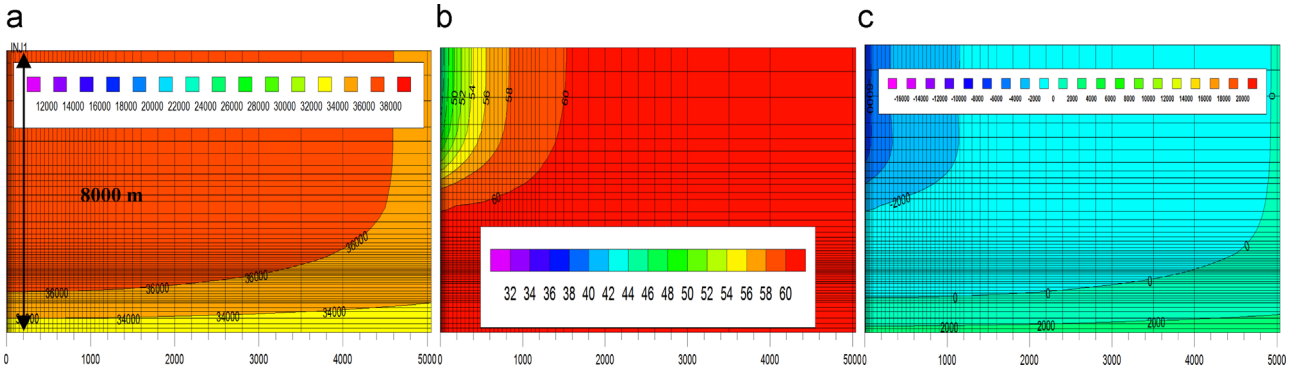

Fig. 12. (a) Pressure distribution (kPa), (b) temperature (°C) and (c) minimum effective stress (kPa) after 30 years of injection for thermal model with 7.2E4 m^3/day injection rate.

storage goal would need drilling more wells in the targeted area. This would increase the drilling cost while heating or cooling CO_2 also changes costs for the storage project. These factors will potentially play an important role in economics of a storage project. Fig. 14 depicts this optimization algorithm.

The algorithm in Fig. 14 is used in this study for optimizing the storage based on the injection rate and temperature. The goal is to inject CO_2 for a period of 10 years in the Rose Run sandstone aquifer by allowing drilling multiple wells and keeping a maximum fracture length of 150 m for each well during operation. The storage area is divided into smaller sectors limited to maximum size of the allowed fracture length (150 m) and the injection rate for each sector is determined based on two criteria: maximum injected volume of CO_2 and maximum allowed fracture length of 150 m. The selected maximum fracture length of 150 m is arbitrary and based on the assumed well spacing in this study. The idea is to avoid interference between induced fractures. Fig. 15 shows a schematic of the developed quarter element of symmetry model with the injection well on the top left corner and the extension to the full field representation.

It is important to note that due to the existing significant stress contrast between the reservoir and caprock, vertical propagation of fracture is limited to the reservoir. Therefore in all of the optimization cases, the security of storage is assumed to be maintained while the efficiency of storage is maximized due to the higher well injectivities resulting from induced fractures.

CO_2's transportation temperature and pressure is reported to generally vary between 4 and 38 °C and 8619 and 15,300 kPa respectively. The lower end of the pressure range is for avoiding two-phase flow in the pipeline and the higher end is for economic concerns. The lower limit in the temperature range is set by the ground temperature in the winter and the higher limit is affected by the temperature of the compressor station and the thermal limit of the pipeline coating material (Mohitpour et al., 2003).

The operating temperature range is lower than the typical reservoir or aquifer temperature. Therefore thermal effects are expected to reduce injectivity at small injection rates unless CO_2's temperature is raised before injection or CO_2 is transported at higher temperature. Transporting CO_2 at higher temperature reduces the flow capacity of the pipeline unless pipeline's diameter is fairly large which results in higher transportation cost. Also using pipelines with large diameters in the design reduces the number of usable built-in CO_2 or natural gas pipelines for CCS projects. For that reason, and since the optimum way to transport CO_2 is in a dense phase or supercritical fluid (IEA Greenhouse Gas R&D Program, 2005), we have assumed that the CO_2 will be delivered to the wellhead in dense phase. The assumed temperature and pressure of the delivered CO_2 is 5 °C and 10,000 kPa. These parameters are in the range reported above for delivered CO_2 in dense liquid phase. Based on this assumption, CO_2 has to be pressurized and heated before injection if the project is designed such that thermal effects are avoided. This will require using high pressure pumps and heaters at the well head.

The cost analysis in this study (based on presented optimization algorithm) has three main parts: pumping, heating, and well drilling cost. The drilling cost is assumed to be \$4E+06 for each well (Lucier and Zoback, 2008). The cost for each well should be first calculated based on the injection parameters and then multiplied by the number of wells (sectors) necessary to deliver desired field injection rate to determine the overall cost.

Pumping cost in each sector is a function of the pumping pressure and is calculated as below:

$$\$C_{pump} = \frac{Q_{cum}\,\Delta P}{\eta_p}\$C_{energy} \quad (1)$$

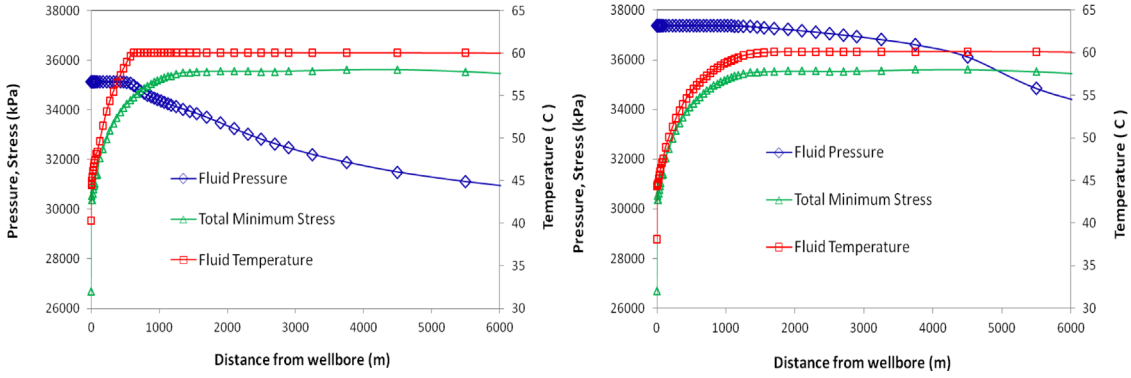

Fig. 13. Total stress , pressure and temperature distribution in the fracture plane for the thermal model with 4.5E4 m^3/day injection rate (left) and 7.2E4 m^3/day injection rate (right).

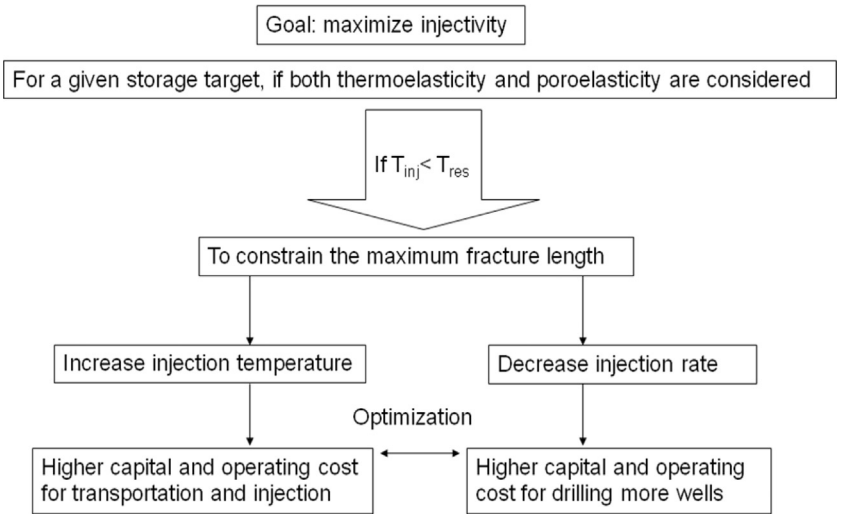

Fig. 14. The proposed storage optimization algorithm as a function of injection rate and temperature.

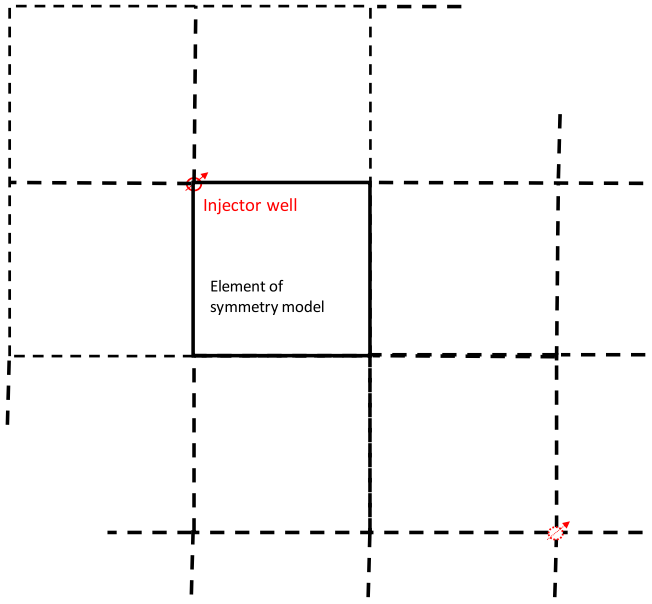

Fig. 15. A schematic of the developed quarter element of symmetry model with the injection well on the top left corner and the extension to the full field representation.

Here, $\$C_{pump}$ is the pumping costs for each sector, Q_{cum} is total injected volume in each sector, ΔP is the pressure difference between the wellhead and the delivered pressure of CO_2, and η_p is pump efficiency, $\$C_{energy}$ is the energy costs.

The heating cost is calculated based on the temperature difference between the injected and delivered temperature of CO_2 to the wellhead. The pump efficiency was assumed to be equal to 1 in this study.

$$\$C_{heating} = \frac{Q_{cum}\rho C_p \Delta T}{\eta_T}\$C_{energy} \quad (2)$$

where, $\$C_{heating}$ is the heating costs, ρ is density, C_p is the heating capacity of CO_2 at supercritical condition, ΔT is the temperature difference between the injection and the delivered temperature of CO_2, and η_T is the thermal efficiency of the heater. The thermal efficiency of the heater was assumed to be 1 in this study.

Average CO_2 heating capacity over temperature range of 30–60 °C is assumed as 0.87 Kj/kg K (Span and Wagner, 1996). Energy cost for calculation of pumping and heating cost is assumed to be 97.3 cents/Kwh. This is the average commercial price in 2010 for the state of Ohio (U.S. Energy Information Administration, 2012).

The total injected volume is a critical variable for determining the overall cost in each sector which is influenced by the induced length of fracture. In order to determine the maximum allowable injection rate, the coupled thermal and geomechanical model of CO_2 injection in Rose Run aquifer was run with different injection rates and temperatures. Fig. 16 shows the propagation of fracture as time progresses for different injection rates and different temperature differences ΔT between the reservoir and injected CO_2.

If a maximum fracture length of 150 m is allowed, for each ΔT, a maximum injection rate can be determined from each graph and used for the calculation of the total cost. Fig. 17 shows the variation of the total cost per 1 m^3 of stored CO_2 in each sector as a function of temperature difference between reservoir and injected CO_2 (based on the above mentioned assumption for temperature and pressure of the delivered CO_2). As can be seen in the graph, for our base case scenario, the optimal scenario is to inject CO_2 at the delivered temperature. It should be noted that the resulting optimum strongly depends on the assumptions in calculating different components of the total storage cost. For the particular assumptions in this study, the variation in the total cost is strongly affected by the variation in heating cost. For small targeted temperature difference between the injected CO_2 and reservoir (i.e., $\Delta T = 0, 15$), the heating cost increases (due to heating CO_2 to desired temperature) and results in higher total cost. As the targeted temperature difference increases (i.e., $\Delta T = 30, 55$), since less heat is required, heating cost drops and the pumping and drilling cost becomes dominant. These two types of cost depend on the allowable injection rate which is constrained based on keeping a maximum fracture length of 150 m. As seen in Fig. 16 , the difference between allowable rate for $\Delta T = 30$ and 55 °C is very small and the reason for this is that the effect of ΔT on thermoelastic effects of cold injection becomes small beyond a certain ΔT. Therefore since the allowable injection rates are not very different between $\Delta T = 30$ and 55 °C, the pumping and drilling costs for these two cases are similar. In the absence of large heating costs, this explains the lack of variation of total cost between cases with $\Delta T = 30$ and 55 °C.

As noted before, the resulting optimum scenario strongly depends on the assumptions in calculating different components of the total storage cost. As an example, if the well drilling cost would be an order of magnitude larger, the cost effective storage scenario would be to heat the delivered CO_2 to 30 °C before injection (Fig. 17).

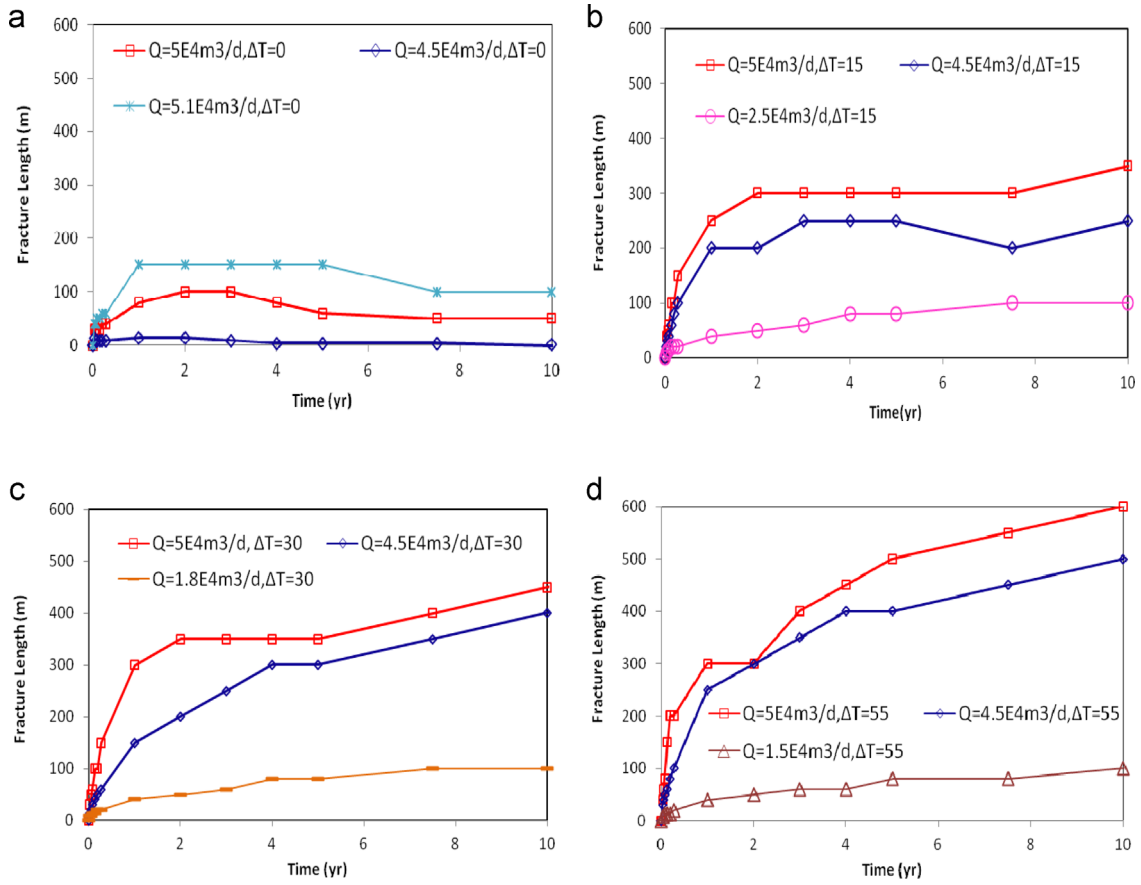

Fig. 16. Fracture length for the thermal model with different injection rates at (a) zero, (b) 15 °C, (c) 30 °C and (d) 55 °C temperature gap between reservoir and injected CO_2.

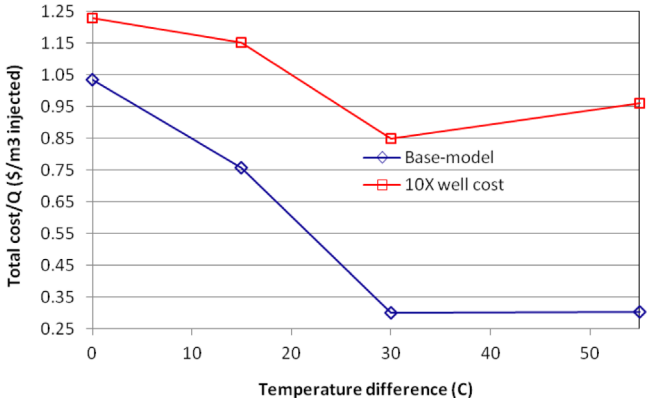

Fig. 17. Total cost for 1 m^3 of stored CO_2 as a function of temperature difference between reservoir and injected CO_2 and total injected volume shown for two models with different drilling associated costs.

This paper was focused on the proposed algorithm for optimizing the storage capacity from a thermal and geomechanics perspective. The cost analysis presented is relatively simplified and the method and values used for determination of the total cost could significantly change based on project design. Therefore the presented algorithm should be used with the cost analysis specific to the CCS project to be optimized with respect to storage capacity.

9. Conclusions

This work investigated the thermal effects of CO_2 injection using vertical wells for CO_2 storage using coupled fluid flow and heat transfer, geomechanics and fracturing simulation. Injecting CO_2 at a temperature lower than reservoir temperature reduces the fracture pressure which results in smaller injection capacity. Therefore coupling heat transfer model with flow and geoemchanical model is necessary for accurate simulation of CO_2 storage geomechanics. In risk assessment studies inclusion of the thermal effects will therefore help prevent the unexpected leakage in storage projects.

As the injection rate increases, thermal effects of injection on fracture propagation decrease, but tendency for fracturing increases regardless of thermal effects. At small enough injection rates, fracture propagation is controlled primarily by the injection temperature, and is accelerated as injection temperature is decreased. As a result, spontaneous fracturing is expected to take place in most CCS projects that use vertical wells with injection temperature below reservoir temperature, unless the injection rates are impractically low. This is an important finding which will also have consequences for caprock integrity.

The dependence of fracture propagation and fracturing pressure on injection temperature opens interesting possibilities for optimization of CCS projects. The optimization process should consider as variables: injection rate and temperature, well spacing and number of wells needed and associated capital and operating costs of CO_2 heating/cooling and pipeline and injection equipment.

An optimization algorithm has been proposed and used to determine the cost effective storage scenario for the CO_2 injection in the Rose Run sandstone aquifer in Ohio River Valley. The optimal cost effective solution was found to be a function of the difference between the temperature of the reservoir and injected CO_2 and the components of drilling associated cost. The methodology developed will play an important role in process optimization for maximizing the injection capacity while maintaining the safety of storage.

The work needs to be extended for horizontal wells, because the well geometry will have a large effect both on fracture behavior and project optimization.

Acknowledgments

Funding for this study was provided through Institute for Sustainable Energy, Environment, and Economy (ISEEE) and TAURUS Reservoir Solutions Ltd.

References

Bissell, R.C., Vasco, D.W., Atbi, M., Hamdani, M., Okwelegbe, M., Goldwater, M.H., 2011. A full field simulation of the In Salah gas production and CO_2 storage project using a coupled geo-mechanical and thermal fluid Flow simulator. Energy Proc. 4, 3290–3297.

Collieu, A. Mc.B., Powney, D.J., Girifalco, L.A., et al., 1975. The mechanical and thermal properties of materials and statistical physics of materials. Phys. Today 28, 51.

Fjaer, E., Holt, R.M., Horsrud, P., et al., 2008. Petroleum Related Rock Mechanics. Elsevier, p. 441.

Goodarzi, S., Settari, A., Keith, D., 2012. Geomechanical modeling for CO_2 storage in Nisku aquifer in Wabamun Lake area in Canada. Int. J. Greenh. Gas Control 10, 113–122. http://dx.doi.org/10.1016/j.ijggc.2012.05.020, ISSN: 1750-5836.

Goodarzi, S., Settari, A., Zoback, M., et al., 2011. A coupled geomechanical reservoir simulation analysis of CO_2 storage in a saline aquifer in the Ohio River Valley. Environ. Geosci. J. Am. Asso. Pet. Geol. 18 (3), 1–20.

Goodarzi, S., Settari, A., Zoback, M., Keith, D., 2013. Thermal effects on shear fracturing and injectivity during CO_2 storage. Effect. Sustain. Hydraul. Fract. . http://dx.doi.org/10.5772/56311, ISBN: 978-953-51-1137-5, InTechhttp://www.intechopen.com/books/effective-and-sustainable-hydraulic-fracturing/thermal-effects-on-shear-fracturing-and-injectivity-during-CO2-storage

Gor, G.Y., Elliot, T.R., Prevost, J.H., 2013. Effects of thermal stresses on caprock integrity during CO_2 storage. Int. J. Greenh. Gas Control 12, 300–309.

Guildner, L.A., 1958. The thermal conductivity of carbon dioxide in the region of the critical point. Proc. Natl. Acad. Sci. USA 44 (11), 1149–1153.

Gupta, N., 2008, Topical Report: The Ohio River Valley CO2 storage project AEP Mountaineer Plant West Virginia-Characterization of potential for geologic storage of CO2 project#DE-AC26-98FT40418,Battelle,Columbus, Ohio.

Hassanzadeh, H., Pooladi-Darvish, M., Elsharkawy, A.M., Keith, D.W., Leonenko, Y., 2008. Predicting PVT data for CO_2-brine mixtures for black-oil simulation of CO_2 geological storage. Int. J. Greenh. Gas Control 2 (1), 65–77.

IEA Greenhouse Gas R&D Programme, 2005. Building the cost curves for CO_2 storage: European Sector, Report no. 2005/2.

Ji, L. , Settari, A., Sullivan, R.B., Orr, D., 2004.:"Methods For Modeling Dynamic Fractures In Coupled Reservoir And Geomechanics Simulation", Paper SPE 90874, presented at the SPE Annual Technical Conference and Exhibition, Houston, TX.

Lucier, A., Zoback, M., Gupta, N., et al., 2006. Geomechanical aspects of CO_2 sequestration in a deep saline reservoir in the Ohio River Valley region. Environ. Geosci. 13 (2), 85–103.

Lucier, A., Zoback, M., 2008. Assessing the economic feasibility of regional deep saline aquifer CO_2 injection and storage: a geomechanics-based workflow applied to the Rose Run sandstone in Eastern Ohio, USA. Int. J. Greenh. Gas Control 2 (2008), 230–247.

Mohitpour, M., Golshan, H., Murray, A., 2003. Pipeline Design & Construction: A Practical Approach, third ed. ASME Press, NewYork, NY, p. 556.

Peters, E., Pizzocolo, D., Loeve, P.A., Fokker, C., Hofstee, B., Orlic, J.G., 2013. Maas Consequences of thermal fracture development of cold CO_2 into depleted gas fields Greenhouse Gas Control Technologies 12. In: Proceedings of the 12th International Conference on Greenhouse Gas Control Technologies (GHGT-12), Elsevier.

Preston, C., Monea, M., Jazrawi, et al., 2005. IEA GHG Weyburn CO_2 monitoring and storage project. Fuel Process. Technol. 86, 1547–1568.

Rayward-Smith, W.J. and Woods, A.W. (2011). Some implications of cold CO2 injection into deep saline aquifers. Geophysical Research Letters 38: doi: 10.1029/2010GL046412. issn: 0094-8276.

Rutqvist, J., 2012. The geomechanics of CO_2 storage in deep sedimentary formations. Int. J. Geotech. Geol. Eng. . http://dx.doi.org/10.1007/s10706-011-9491-0 30:525–551

Silva, O, Vilarrasa V, Carrera J., 2011. An efficient injection concept for CO2 geological storage. 6th Trondheim Carbon, Capture and Sequestration Conference, 14-16 June, Trondheim, Norway.

Settari, A., Walters, D.A., 2001. Advances in coupled geomechanical and reservoir modeling with applications to reservoir compaction. SPE J. 6 (3), 334–342.

Settari, A., Warren, G.M., 1994. Simulation and field analysis of waterflood induced fracturing. Paper SPE 28081. Proceedings, SPE/ISRM Meeting. Rock Mechanics in Petroleum Engineering. Delft, pp. 435–445.

Solomon, S., 2006. Carbon Dioxide Storag e: Geological Security and Environmental Issues-Case Study on the Sleipner Gas Field in Norway The Bellona Foundation.

Span, R., Wagner, W., 1996. A new equation of state for carbon dioxide covering the fluid region from the triple-point temperature to 1100 K at Pressures up to 800 MPa. J. Phys. Chern. Ref. Data 25 (6).

Taurus, 2015. ⟨http://www.taurusrs.com/geosim.html⟩.

U.S. Energy Information Administration, 2012. State Electricity Profiles 2010. Assistant Administrator for Energy Statistics Office of Electricity. Renewables, and Uranium Statistics U.S. Department of Energy Washington, DC 20585, DOE/EIA-0348(01)/2, (released 27.01.12), p. 215.

van Genuchten, M.T., 1980, A closed-form equation for predicting the hydraulic conductivity of unsaturated soils: Soil Science Society of America Journal v. 44/5, p. 892-898.

Vilarrasa, V., Olivella, S., Carrera, J. and Rutqvist, J.: Long term impacts of cold CO2 injection on the caprock integrity, International Journal of Greenhouse Gas Control, 24, (2014), 1-13.

Wright, L.W., 2007. The In Salah Gas CO_2 Storage Project International Petroleum Technology Conference.

Yaws, C., 2008. Thermophysical Properties of Chemicals and Hydrocarbons. 793. William Andrew Publishing, p. 799.

Zoback, M.D., Zoback, M.L., 1981. State of stress and intraplate earthquakes in the central and eastern United States. Science 213, 96–109.